Desalination and Water Treatment
www.deswater.com
doi: 10.1080/19443994.2016.1157765

57 (2016) 25972–25984
November

Taylor & Francis
Taylor & Francis Group

Application of an airlift reactor with a net draft tube in phenol bio-oxidation using *Ralstonia eutropha*

Saba Ranjbar[a], Hoda Khesali Aghtaei[a], Elham Jalilnejad[b], Farzaneh Vahabzadeh[a,*]

[a]*Chemical Engineering Department, Amirkabir University of Technology (Tehran Polytechnic), 424 Hafez Ave., Tehran, Iran, Tel. +98 21 64543161; Fax: +98 21 66403180; emails: Saba.r@aut.ac.ir (S. Ranjbar), Hoda.khesali@aut.ac.ir (H. Khesali Aghtaei), Tel. +98 21 64543161; Fax: +98 21 66405847; email: Far@aut.ac.ir (F. Vahabzadeh)*
[b]*Chemical Engineering Department, Urmia University of Technology, Urmia, Iran, Tel. +98 44 31980299; email: E.jalilnejad@uut.ac.ir*

Received 16 September 2015; Accepted 17 February 2016

ABSTRACT

Phenol biodegradation by *Ralstonia eutropha* was studied in a constructed airlift reactor with a stainless steel net draft tube (ALR-NDT). In giving a description of the cell performance, it is necessary to quantify the relationships between the bioreactor characteristics (gas holdup (ε_G), time of mixing (t_m), and gas–liquid mass transfer coefficient (K_La)) and the cell bioprocesses. Thus, the hydrodynamic properties of the reactor were measured using air–water and air–mineral salt solution (MSS) systems. The K_La value for the MSS system in ALR-NDT was 1.2 times higher than the bubble column reactor and airlift reactor as modified versions of the ALR-NDT. Improvement in t_m was also considerable for air–MSS in the ALR-NDT. At higher superficial gas velocities (U_Gs), ALR-NDT performance was better in terms of ε_G obtained for air–MSS compared with an air–water system. Growth and phenol consumption by *R. eutropha* followed substrate inhibition kinetics, and the experimental data for the specific growth rates at three different U_Gs were fitted to the Haldane, Edwards and Aiba–Edwards models. Between these models, the latter gave the best fit according to the goodness of fit results. The estimated kinetic parameters were indicative of a high potential for *R. eutropha* in degrading phenol.

Keywords: Airlift reactor with net draft tube; Gas holdup; Gas–liquid mass transfer coefficient; Growth kinetics; *Ralstonia eutropha*

1. Introduction

The presence of phenol in industrial wastewaters is common, and this structurally simple aromatic compound has been used in the production of a variety of chemicals as a raw material; however, natural phenolic sources (i.e. plant phenolics) contain phenol at much lower concentrations. Diversity of the involved ecosystems for phenol is thus high, and the environmental burden of this organic pollutant is a challenge. The popularity of bio-based technologies has steadily increased in the past decades, mainly because of the eco-friendly properties of these techniques, including energy requirements and process economics [1–3]. *Ralstonia eutropha* is capable of consuming and degrading a variety of xenobiotic organic pollutants [1,3]. Different environmental factors and their interactions

*Corresponding author.

affect the kinetics of biodegradation of a particular substrate, but the likeliness of predicting the cell behavior and kinetics of degradation has been considerably reduced because of the complex nature of the microbes [4,5]. Special attention has been directed toward growth under substrate inhibition conditions, where different mathematical models have been used to describe the cell behavior [6].

Tower-type reactors have gained interest for their applications in aerobic biochemical fermentations, and these pneumatically agitated reactors gain the kinetic energy of the input gas for liquid circulation and mixing of the reactor content [7,8]. The pattern of fluid flow is the main difference between the bubble column reactor (BCR) and airlift reactor (ALR); in the former, the medium in the vessel is randomly mixed by ascending air bubbles, whereas gas sparging at the bottom region of the riser is used in an ALR, and the differences of gas holdup (ε_G) between this part and the downcomer section creates a pressure difference, which forces liquid to move (from the bottom of the downcomer to the riser) and circulate in a special pattern in the vessel (fluid flow under the influence of the reactor geometry) [9,10]. The energy in BCR is high at the point of introducing gas into the system, and the energy decreases with distance. This energy dissipation damages the medium contents, including microbial cells. The advantage of ALR is due to receiving energy uniformly throughout the system for the fluid to flow [10–12]. Further improvement of ALR performance was achieved by introducing a net draft tube to the reactor: the efficiency of liquid mixing was achieved by shortening the time of mixing and a higher oxygen transfer rate was obtained due to prevalence of homogenous bubbly flow regime in the system [8].

The functionality of phenol-2-monooxygenase (1.14.13.7) as a hydroxylating enzyme in the 1.14 subgroup depends on NAD(P)H coenzyme as one of the two hydrogen donors required for oxidative biocatalysis. However, the limited stability of these coenzymes outside microbial cells restricts the use of the pure enzymes, especially in environmental applications, and has generated great attention to the use of whole cells as biocatalysts: access to sustainable, oxygenase-based, whole-cell biocatalysis is a promising approach [13,14]. Based on the results obtained previously in our laboratory, attempts were made to study the use of *R. eutropha* as a whole-cell biocatalyst for the bio-oxidation of phenol in an airlift reactor with a net draft tube (ALR-NDT), where the hydrodynamic behavior of the reactor and oxygen mass transfer effects were characterized using air–water and air–mineral salt solution (MSS) systems [3,15,16]. The performance of the ALR-NDT was compared with the performance of two different reactor configurations: BCR and ALR. Three different superficial air velocities (0.94, 2.82, and 5.64 cm/s) were used to study phenol bio-oxidation, and to explain the cell growth kinetics, three different substrate inhibition models were used, namely, Haldane, Edwards, and Aiba–Edwards. Evaluation of the kinetic parameters and testing of the quality of the experimental data fitting to the models were conducted using a nonlinear regression technique.

2. Materials and methods

2.1. Microorganism and cultivation

The bacterium *R. eutropha* (PTCC 1615) was obtained from the Persian Type Culture Collection (Iranian Research Organization for Science and Technology "IROST", Tehran, Iran) in lyophilized form. The phenol-oxidizing ability of the test bacterium was due to the acclimatization process, which has been conducted previously in our laboratory, and details can be found in the relevant references [3]. The constituents of the mineral salt solution (MSS) were (g/L dis H_2O): 1 g/L K_2HPO_4, 1 g/L KH_2PO_4, 1 g/L $(NH_4)_2SO_4$, and 0.05 g/L $MgSO_4{\cdot}7H_2O$. After adjustment of the pH of the MSS to 7 using 1 N NaOH solution, the medium was sterilized in an autoclave (121°C-20 min). *R. eutropha* cell suspension having OD = 0.5 and at 10% v/v was cultivated in a 250-mL Erlenmeyer flask containing 90 mL of MSS to which 0.02 g phenol was added, and the culture was incubated in a shaker incubator (Kühner, Switzerland) at 150 rpm, 30°C for 24 h.

2.2. ALR-NDT operation

To determine the hydrodynamic behavior of the ALR-NDT (gas holdup "ε_G", mixing time "t_m", and volumetric gas liquid mass transfer coefficient "K_La"), experiments were performed in a previously constructed reactor used in our laboratory [7]. The detailed description of the geometrical characteristics of reactor is given in Fig. 1 legend. With the net draft tube removed from the glass cylindrical vessel, the reactor was characterized as a BCR, and with the use of the solid draft tube, the reactor behavior was evaluated as an ALR (Fig. 1). Hydrodynamics and mass transfer studies on these test reactors were performed using air–water and air–MSS system. The related experiments were performed in the absence of the test bacterium and phenol. In the biodegradation experiments, the ALR-NDT was filled with 540 mL of MSS containing 10% v/v (OD = 0.5) of the bacterium culture. Phenol was used as the sole substrate for *R.*

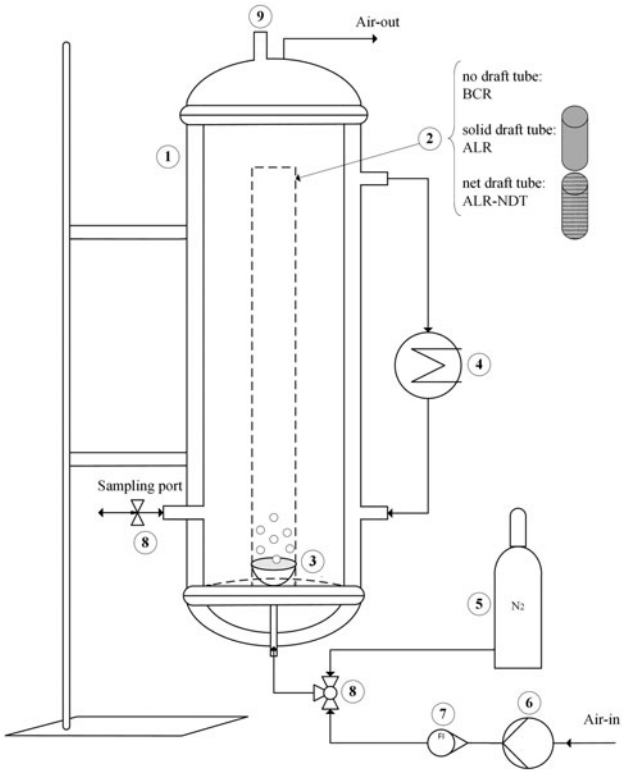

Fig. 1. Arrangement of the bioreactor used in the present study.
Notes: (1) bioreactor (height = 42 cm and ID = 5 cm, 825-mL glass cylindrical vessel with a working volume of 540 mL); (2) Draft tube (internal concentric net draft tube made of stainless steel with height = 25 cm and ID = 1.5 cm, placed 10 cm above the bottom of the glass vessel). Without the draft tube, the reactor performed as a BCR, and with a solid draft tube, the reactor performed as an ALR; (3) sintered glass sparger (with 10 holes each having 0.1 mm diameter); (4) thermostatic pump connected to the jacket of the cylindrical glass vessel; (5) N_2 cylinder; (6) aquarium air pump; (7) rotameter; (8) valve; (9) DO meter and conductometer plug-in.

eutropha growth, and it was added to the test bioreactor at six different initial concentrations, ranging from 25 to 600 mg/L (all experiments were performed at 30°C).

2.3. Analytical techniques

Two parts are presented in this section. In the first, the fluid flow in the ALR-NDT was characterized by measuring ε_G, t_m, and oxygen mass transfer considering five different U_Gs. By dividing the volumetric gas flow rates (cm^3/min) by the cross-sectional area of the riser, the target values for the U_Gs were obtained (e.g. $U_g = \frac{100\,(cm^3/min)}{1.77\,(cm^2)\times 60\,(S)} = 0.94$ (cm/s), which is equal to an aeration rate of 0.18 (vvm)).

In the second part, the measuring methods were extended to monitor the changes of the phenol concentration and biomass content during the biodegradation process.

Meanwhile, the density and surface tension of the individual components of the MSS were determined according to the standard methods. For instance, a Wilhelmy plate, as a tensiometer, was used to measure the surface tension (Kruss tensiometer k14).

2.3.1. Gas holdup (ε_G)

According to the volume expansion method described in the literature [12] in terms of the liquid height in the reactor which changes with the system's aeration, the following expression was used in the present study for determination of ε_G (Eq. (1)):

$$\varepsilon_G = \frac{V_{f-}V_i}{V_f} = \frac{H_{LG} - H_L}{H_{LG}} \quad (1)$$

where H_L is unaerated liquid height or (V_f as the corresponded volume) in the reactor and H_{LG} is the aerated height of the liquid (or V_i as corresponded the volume) [8]. The ε_G measurements in the test reactors were repeated ten times.

2.3.2. Mixing time (t_m)

Determination of the t_m was performed according to the conductometry procedure described by Hsiun and Wu, where 4 M NaCl solution as the tracer for a pulse test was added from the sampling port, as shown in Fig. 1. The volume of the NaCl solution used in this measurement was 1/1,000 based on the working volume of the reactor. The t_m was defined as the time required for the probe response curve to reach 95% of the final tracer conductivity [17].

2.3.3. Volumetric gas–liquid mass transfer coefficient (K_La)

In dynamic K_La measurement, a common technique is to monitor the oxygen profile by first introducing N_2 gas and deoxygenating the reactor content and admitting air at a fixed rate (gassing out–gassing in method) [18]. By using a dissolved oxygen (DO) electrode (Oxi 340i/SET, WTW, Germany), the variation of the DO in the reactor was recorded. The K_La values were calculated using Eq. (2), where C_0, C_s, and C are the initial, saturated, and bulk concentrations of DO, respectively [19]:

$$K_L a = \frac{\ln(1-\frac{C-C_0}{C_s-C_0})}{t-t_0} \quad (2)$$

The DO measurements in the test reactors were repeated five times.

2.3.4. Phenol and biomass contents

The contents of phenol and biomass were measured spectrophotometrically (V-550 UV–vis spectrophotometer, Jasco, USA), and the value of the latter was obtained by reading the absorbance of a sample solution at 600 nm (the samples were taken at regular time intervals). A calibration curve was used in correlating the OD to the dry cell weight [3]. The sample solution was then centrifuged at 8,000 rpm for 15 min. By adding Folin–Ciocalteau reagent to the supernatant and following the details of the relevant method, the phenol content was determined by obtaining the absorbance at 750 nm [20].

2.4. Data analysis

Fitting of the experimental data to the models that are nonlinear for each parameter was performed by nonlinear regression using the Levenberg–Marquardt algorithm (GraphPad Prism 5 software). This work requires an initial estimate of the parameters of interest, and the program, after many iterations, automatically calculates the lowest values of the sum of squares of the differences between the model-predicted values ($\hat{y}$) and the experimentally obtained data (y) (minimization of the sum of squares of the residuals "SSR") considering the gradient descent and Gauss–Newton methods. The standard error of the estimate about parameter ($S_{y.x}$) can be described using Eq. (3), where df is equal to number of data points minus the number of parameters fit.

$$S_{y.x} = \sqrt{\frac{SSR}{df}} = \sqrt{\frac{\sum(y-\hat{y})^2}{df}} \quad (3)$$

The coefficient of determination (R^2) gives the proportion of the total variability of data explained by the model (Eq. (4)) (where $\sum(y-\hat{y})$ is the total variability in y about the sample mean) [21].

$$R^2 = 1 - \frac{\sum(y-\hat{y})^2}{\sum(y-\bar{y})^2} \quad (4)$$

Thus, the quality of the data fitting to the test models has been reported as the goodness of fit values ($S_{y.x}$ and R^2).

3. Results and discussion

3.1. Hydrodynamic characterization and oxygen mass transfer

The experiments were conducted in the test reactor (see Fig. 1 for the reactor details). The air flow rate and liquid phase properties, such as the density and surface tension, affect the reactor performance. These properties are shown in Table 1.

3.1.1. Gas holdup

The gas holdup, as the fraction of the total reactor volume occupied by gas, was measured separately for the air–water and air–MSS systems in the test reactors. Fig. 2 shows the dependence of ε_G on U_G (ranged from 0.94 to 9.44 cm/s). Considering ALR and ALR-NDT at low air flow rate, up to 4.72 cm/s, the ε_G for MSS was lower compared with water, whereas this trend was not seen for the BCR, in which ε_G for MSS and water were comparable at the low air flow rate (<4.72 cm/s) (Fig. 2(a)). Better behavior of BCR in terms of ε_G for air–water compared with ALR and ALR-NDT was also observed by Chen et al. [22]. As

Table 1
Liquid-phase properties

Solution	Density (g/cm^3)	Surface tension (mN/m)
Distilled water	0.9916	72
MSS	0.9969	69
KH_2PO_4 (1 g/L)	0.9927	60
K_2HPO_4 (1 g/L)	0.9925	67
$(NH_4)_2SO_4$ (1 g/L)	0.9925	66
$MgSO_4{\cdot}7H_2O$ (0.05 g/L)	0.9917	66

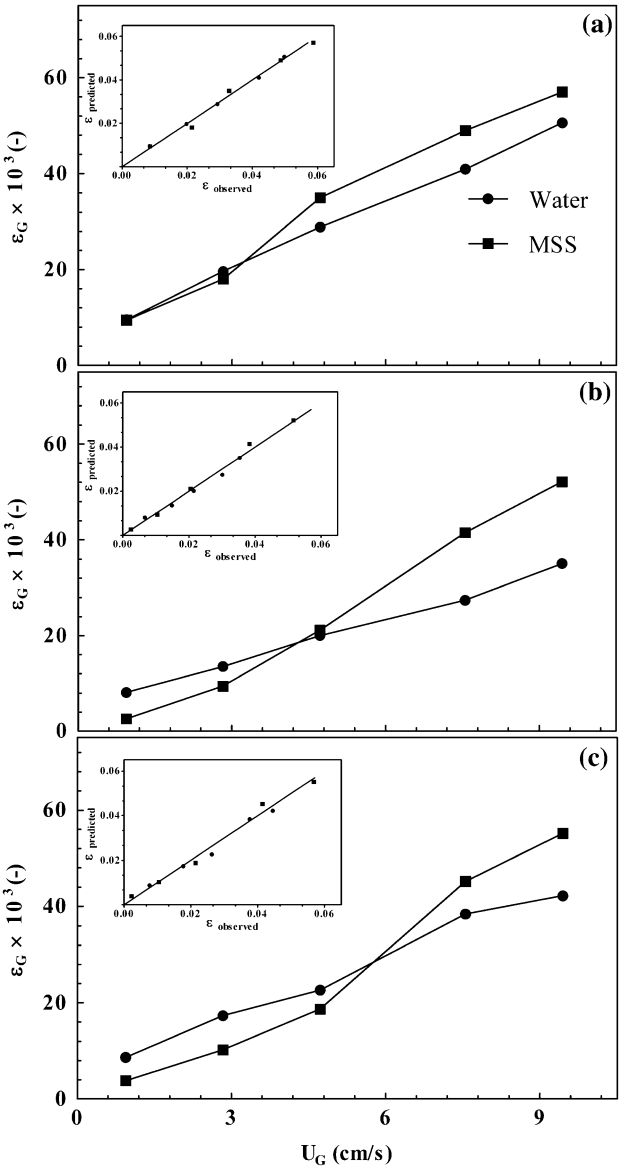

Fig. 2. Gas holdup as a function of the superficial gas velocity for air–water and for the air–MSS system considering the three test reactors: BCR (a), ALR (b) and ALR-NDT (c). The parity plot of the experimental values of the gas holdup for each test reactor using equation $\varepsilon_G = aU_G^n$ is shown in the inset.

seen in Fig. 2, the performance of ALR-NDT for water was better than ALR, and this was in agreement with the findings reported by Wu and Wu [12]. The increasing trend of ε_G with the increase in U_G for MSS above the increasing trend of air–water in BCR started at 4.72 cm/s, where ε_G for MSS at U_G = 9.44 cm/s was approximately 12.6% higher compared with water (Fig. 2(a)). The ε_G difference between MSS and water for ALR at U_G = 9.44 cm/s was the highest (49%), whereas in the case of ALR-NDT, at the same U_G, ε_G for MSS was approximately 31% higher than that of water (Fig. 2(b) and (c)). The relationship between the reduction in the surface tension of solutions of some electrolytes and the increase in gas holdup (compared with water) in the ALR (as seen in Fig. 2(b)) has been reported elsewhere [23]. The present findings confirm the decrease in surface tension for the low concentrations of electrolytes, where the highest decrease was obtained for the pure KH_2PO_4 electrolyte solution (60 vs. 72 mN/m) (Table 1). Moreover, literature studies on the surface tension of inorganic salts show that the surface tension of these salts increases compared with that of pure water [24,25]. The electrolyte concentrations used in the latter studies were high and are not usable in ordinary fermentation processes. Further studies in the literature have been directed toward the inhibiting effect of some inorganic salts on air bubbles coalescence, where the ion–water interactions along with self-diffusion of water molecules play roles in reducing the aggregation of air bubbles (more discussions on this subject are presented in the "Volumetric gas–liquid mass transfer coefficient" section) [26]. The positive effect of the bubbles coalescence-inhibiting property of some inorganic salts on ε_G increase in BCR has attributed to the occurrence of small air bubbles in the circulated electrolytic solution [27]. The formation of air bubbles in column reactors is a complex process that is describable on the basis of several factors, such as reactor geometry, aerator type, air flow rate, and composition and physical properties of the circulated liquid. These experimental variables have controlling effects on the gas holdup character and thus the reactor behavior.

Attempts were directed toward expressing a correlation between the ε_G and the superficial gas velocity. The use of the $\varepsilon_G \propto U_G^n$ expression is a familiar approach in showing the dependence of ε_G on U_G, where the value of "n" in the exponent gives an impression of the flow regime [28,29]. Table 2 shows the positive effect of MSS on the reactor performance in terms of ε_G as a function of U_G. The improvement for the BCR in terms of the "n" value of the $\varepsilon_G = aU_G^n$ equation (Eq. (5)) is approximately 9% compared with the ε_G character for air–water. The increase in the "n" value was approximately 60–69% for ALR and ALR-NDT compared with those for air–water (Table 2). These findings confirm the results presented in Fig. 2. The different applications of equation one include the results reported by Tung et al.; Nikakhtari and Hill who obtained different values for the "a" coefficient and exponent "n" for different systems [28,29]. In the latter study, a woven stainless steel mesh was used as the packing material, and Nikakhtari and Hill's

Table 2
The correlation between the gas holdup and superficial gas velocity using equation $\varepsilon_G = aU_G^n$

	$\varepsilon_G = aU_G^n$							
	Air–water system				Air–MSS system			
Reactor type	a	n	$S_{y.x}$	R^2	a	n	$S_{y.x}$	R^2
BCR	0.009	0.767	0.0010	0.99	0.009	0.835	0.0025	0.99
ALR	0.007	0.722	0.0015	0.98	0.003	1.331	0.0015	0.99
ALR-NDT	0.008	0.765	0.0022	0.98	0.002	1.409	0.0030	0.99

Note: GraphPad Prism 5 software was used for the data analysis.

findings showed that this system provided negligible resistance to fluid flow and the mass transfer rate [28]. In the present study, high values of exponent of approximately 0.7–1.2 indicate dominance of bubbly flow in the system and low values (0.4–0.7) indicate a lower effect of U_G on ε_G (in the heterogeneous regime and during the transition situations between fluid regimes) as mentioned in the relevant literature [9].

The values of $S_{y.x}$ and R^2 given in Table 2 indicate well-behaved Eq. (5) for the data fitting analysis. Parity plots as the insets in Fig. 2 confirmed the findings. The average deviations of the predicted ε_G from the experimentally obtained data were 6.18 and 5.47% for ALR and BCR, respectively, whereas the deviation was 10.71% for ALR-NDT.

3.1.2. Mixing time

The input energy of the admitted air from the air sparger in ALRs, considering the geometric configuration and all the channeling connections in these reactors, can be regarded as a type of force directed toward liquid, which causes it to be regularly distributed with a particular pattern in the system. This fluid recirculation is indicative of effective mixing, where increasing air flow rate will decrease the t_m. Fig. 3 shows the dependence of t_m on U_G. The values of t_m for the air–water system in the three test reactors were higher compared with that of the air–MSS system. The ALR-NDT performed most efficiently, and a marked decrease in t_m of the MSS at high air flow rates was observed (Fig. 3). In ALR-NDT, a part of the gas and liquid goes to the net draft tube, and large air bubbles as a result of the radial flow break into smaller size bubbles. The liquid mixing behavior between reactors is determined by the dimensionless t_m $(1 - t_m/t_{m,BCR})$. The findings reported by Hsiun and Wu showed that the role of NDT in t_m improvement was more considerable in large columns than in small ones [17]. The dimensionless t_m for air–water and air–MSS systems in the present study considering ALR-NDT and ALR is in the range of 0.16–0.33 and 0.05–0.22, respectively.

3.1.3. Volumetric gas–liquid mass transfer coefficient

The volumetric gas liquid mass transfer coefficient (K_La) is a measure of the oxygen mass transfer capability of the reactor to the bulk liquid, including the target substrate and the cells (i.e. the cells respired and being active for oxidation of phenol) [30]. By establishing the steady-state condition, there is equality between the oxygen absorption rate and the oxygen utilization. The relationships between K_La and several variables, such as the amount of biomass, its extent of respiration in phenol oxidation, bulk concentration of phenol and at the cell surface, have been described in the literature [3,30,31]. With reference to the BCR, ALR, and ALR-NDT, the results of K_La dependence on the U_Gs (0.94–9.44 cm/s) for air–water and the air–MSS systems are presented in Fig. 4. At U_G = 9.44 cm/s, the value of K_La obtained for the air–MSS in the ALR-NDT was 1.2 times higher than that in the BCR and ALR, as shown in Fig. 4. The study of the ALR-NDT built by Tung and colleagues using an air–water system showed that at U_G = 5 cm/s (which is 1.8 times lower than the U_G = 9 cm/s used in the present work), the K_La value was 2 times higher than the BCR [29]. The probability of the creation of small-sized air bubbles in the ALR-NDT is high (as compared to that in BCR and ALR), and small-sized bubbles have a better chance to be distributed uniformly in the bulk liquid, which inhibits bubbles coalescence and favors the increase in the gas–liquid interfacial area. Higher K_La values in ALR-NDT cause preference of the ALR-NDT configuration over two other reactors. Nikakhtari and Hill studied an external loop ALR (EL-ALR) and observed that the K_La value at U_G = 0.8 cm/s was 2.5 times higher compared with that in the EL-ALR without packing. These results showed that the improvement of the K_La value was not related only to the increase in U_G, and the reduced

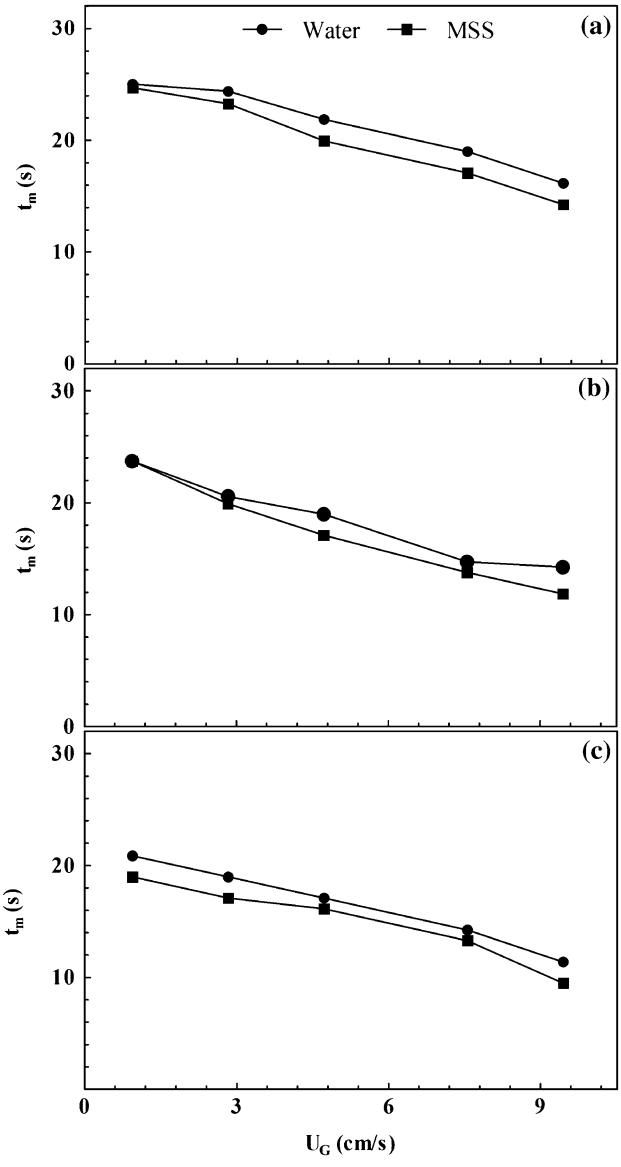

Fig. 3. Mixing time as a function of the superficial gas velocity for the air–water system and for the mineral salt solution for the three test reactors: BCR (a), ALR (b), and ALR-NDT (c).

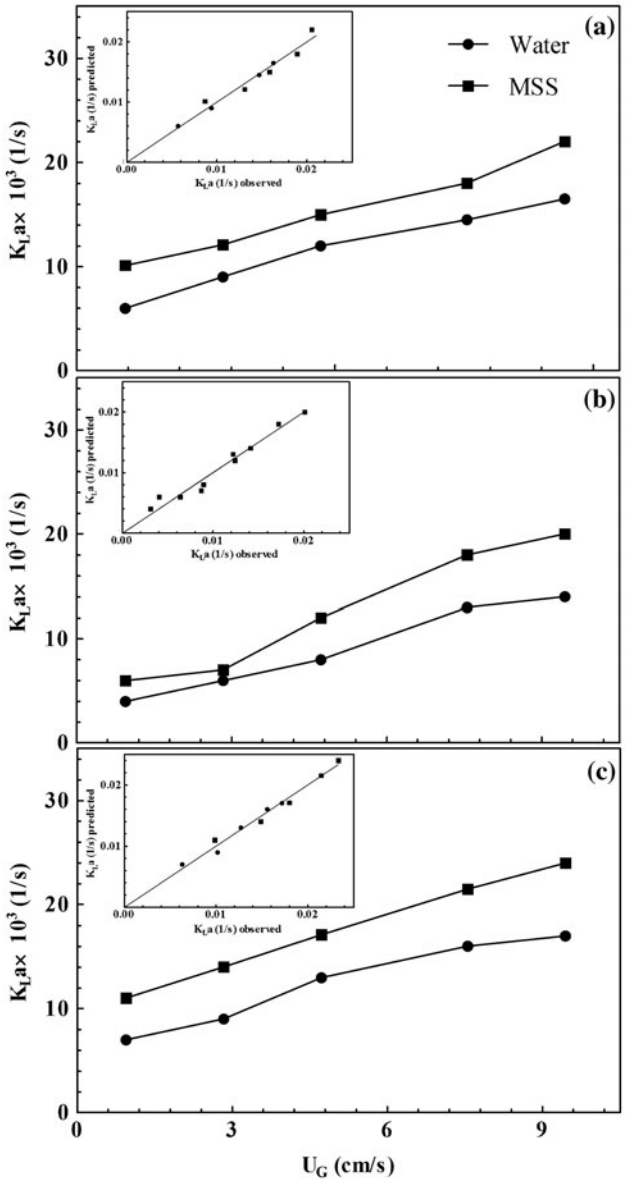

Fig. 4 K_La as a function of the superficial gas velocity for air–water and for the air–MSS system for the three test reactors: BCR (a), ALR (b), and ALR-NDT (c). The parity plot of the experimental values of K_La for each test reactor using equation $K_La = bU_G^m$ is shown in the inset.

limitation of mass transfer effects, the use of packing and its opening size were also important. Because of the air bubble movement toward the downcomer, the researchers did not use high U_Gs beyond 1 cm/s without packing in the EL-ALR [28].

In describing the K_La correlation with U_G, equation $K_La = bU_G^m$ (Eq. (6)) was used, and a linear regression on the data was applied (Table 3). This exponential equation has been used by many researchers, although the values of parameters, including the exponent, in the correlation change as the scale or geometry of the reactor changes [7,28,29]. In expressing the goodness of fit results for the K_La correlation with U_G (Table 3), the parity plots were also drawn, as shown in Fig. 4.

In K_La as a function of U_G, the response of the air–MSS system was much better than that of the air–water, through which the K_La values were 1.17–2.33 times higher than those obtained for the air–water system (Fig. 4). Considering the column reactor and aeration, the ionization of electrolytes in the aqueous system affects the mobility of water molecules around the air

Table 3
The correlation between the K_La and superficial gas velocity using equation $K_La = bU_G^m$

	$K_La = bU_G^m$							
	Air–water system				Air–MSS system			
Reactor type	b	m	$S_{y.x}$	R^2	b	m	$S_{y.x}$	R^2
BCR	0.006	0.457	0.0003	0.99	0.009	0.373	0.0015	0.93
ALR	0.003	0.661	0.0009	0.97	0.004	0.695	0.0016	0.95
ALR-NDT	0.006	0.435	0.0008	0.97	0.001	0.374	0.0010	0.97

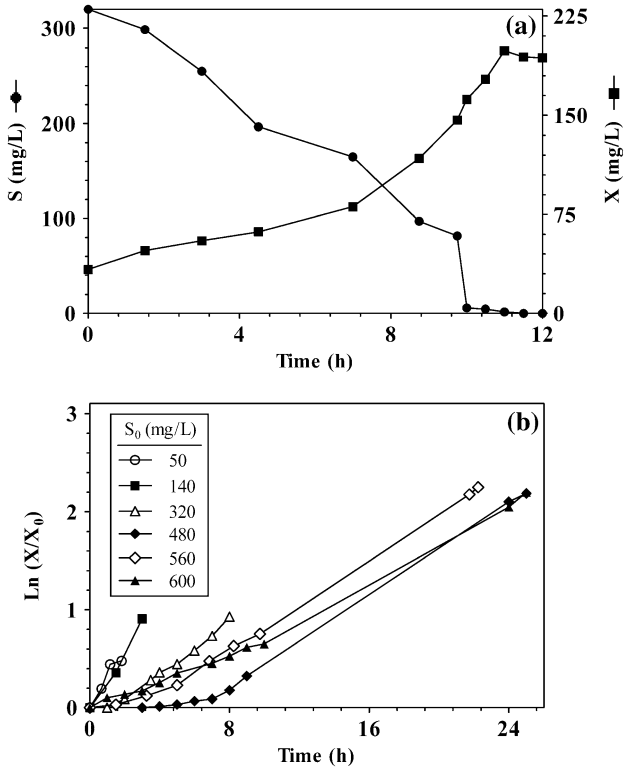

Fig. 5. Changes of the phenol concentration (S) and biomass content (X) as a function of time, measured in the ALR-NDT operating at U_G = 2.82 (cm/s) (a) and *R. eutropha* growth curves as $\ln(x/x_0)$ against time are also shown (b).

bubbles. This behavior is similar to the salting out characteristic of aqueous electrolytic solutions in response to proteins and their isolation [26]. Thus, by participating in breaking hydrogen bonding in water structure, ions play roles in increasing the number of the undissociated water molecules (i.e. the role of ions in solution is the creation of small-sized air bubbles), and these ion–water interactions are responsible for the decrease in air bubble coalescence behavior in ionic solutions [26,27].

3.2. R. eutropha *performance in the ALR-NDT*

With reference to the findings of the ε_G, t_m, and K_La, as have been mentioned in the "Hydrodynamic characterization and oxygen mass transfer" section, the ALR-NDT was the only reactor used in the evaluation of phenol degradative activity of *R. eutropha* in the present work. The preference of ALR-NDT over ALR and BCR is understandable when one considers the ALR-NDT functionality in terms of its capacity for the transfer of oxygen and the mineral nutrients to the *R. eutropha* cells (see Figs. 2, 3 and 4). The oxygen requirement in aerobic phenol biodegradation is describable in terms of the catalytic expression of phenol hydroxylase activity of the test bacterium (see Fig. 4 for the K_La findings vs. U_G) [32].

According to Aiba, if the rate of protein synthesis is the rate-limiting step in the growth, then one may make an analogy between the formation of the complex of the enzyme–substrate (or cell metabolite–substrate) and the amino acid–tRNA–mRNA complex [33]. The cell growth kinetics and the fate of aromatic compound as a consuming substrate has been well studied in the literature [34,35]. The three kinetic models used in the present study were the Haldane, Edwards, and Aiba–Edwards equations, considering the three U_Gs: 0.94, 2.82, and 5.64 cm/s, in the ALR-NDT, and the behavior of *R. eutropha* in growth and the phenol consumption were thus quantitatively described. Fig. 5(a) is an example of the findings in the present work, where data for the time dependence of the biomass growth and phenol consumption by the *R. eutropha* are observable. The specific growth rate, μ, was determined in the first stage of these experiments from the slope of a semi-logarithmic plot of the biomass concentration vs. time for each of the six different initial phenol concentrations (S_0) (Fig. 5(b)). Thereafter, the values of the kinetic parameters for the three models were determined from the plot of μ vs. S_0 using nonlinear regression (see "Data analysis" section) (Fig. 6). In the first portion of the

curves in the figure, μ increases with the increase in the phenol concentration, which is a typical observation for μ compared with the phenol content, where phenol acts as the growth limiting substrate. When $S << K_s$, first-order reaction kinetics apply, and at higher phenol concentrations, the use of the Monod equation is reasonable (Fig. 6(a)). By moving μ from the peak of the curve, phenol acts as the growth-inhibiting substrate (falling portion of the curve is usually concave upward) (Fig. 6). The physiological response of non-axenic soil microbes to the unbalanced nutrient situation in cases of using refractory compound (lack of supportive substrate for the growth) is to excrete partially oxidized substrate, which prevents the intracellular accumulation of suicidal intermediates [32,36]. In ALR-NDT, U_G provides sufficient DO to affect the μ of *R. eutropha* cells and other relevant kinetic parameters, such as K_s and K_i (Table 4). The K_s coefficient is an index of the cell's affinity toward the limiting substrate, showing the amount of substrate needed by the cell to reach $1/2\mu_{max}$. In the present study, the K_s value was the lowest at $U_G = 5.64$ cm/s for the Haldane and Edwards equations. K_i, as an inhibition coefficient is the quantification of toxic compound effect on its biodegradation, and a larger K_i reflects a higher concentration of the substrate to inhibit the cell functionality [37]. The K_i value was the highest at a U_G of 5.64 cm/s using the Haldane model (Table 4). For the Aiba–Edwards equation at $U_G = 0.94$ and 2.82 cm/s, less than 10% difference was obtained between the values of K_s and K_i. The decrease in μ_{max} with the increase in the aeration rate for the Haldane and Edwards equations may indicate cell weaknesses in converting large numbers of phenol molecules per unit time under aerobic conditions. This behavior could be related to the stresses experienced by the cells upon exposure to the unsuitable metabolites, which are likely to be formed faster at higher U_G (such as 2-hydroxymuconate semialdehyde "HMS" formed upon dioxygenase activity on the catechol produced from the enzymatic hydroxylation of phenol) [32]. The toxicity of phenol as a lipophilic compound is related to the negative role of this substance on membrane functionality and the material exchange between the cell and its environment; for instance, in the case of the biphenyl biodegradation study by *R. eutropha*-H850, an increase in the synthesis of saturated fatty acid in the cell membrane due to accumulation of this compound in the cell membrane was observed, which decreased membrane flexibility [38,39]. As shown in Table 4, with the increase in U_G from 0.94 to 2.82 cm/s, for the Haldane model, μ_{max} increased, which may be indicative of the higher affinity of the bacterial cells for phenol as the growth-limiting substrate than phenol as a growth-inhibiting agent (Fig. 6). After increasing U_G from 2.82 to 5.64 cm/s, μ_{max} decreases from 0.772 to 0.430 h^{-1}, and the cells' approach to phenol has physiologically changed from phenol as a growth-limiting substrate to phenol as an inhibitor (Table 4 and Fig. 6). For the Edwards equation, it is important to consider the two

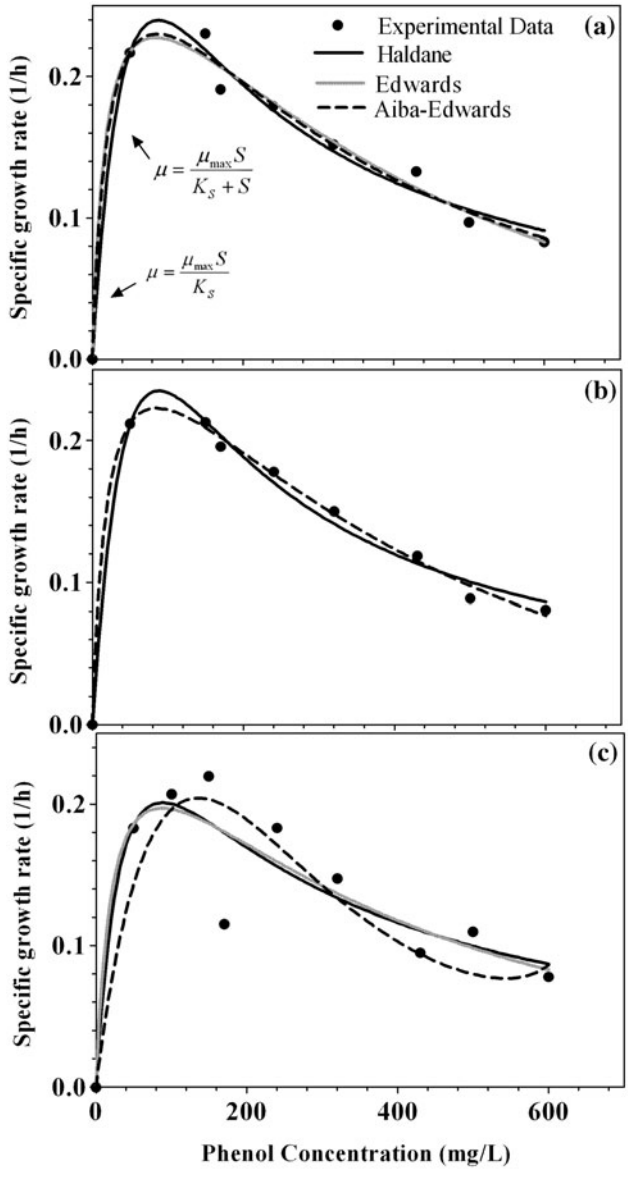

Fig. 6. Specific growth curve as a function of the initial concentration of the phenol substrate. The experimental values were obtained in the ALR-NDT at the three different superficial gas velocities (cm/s): $U_G = 0.94$ (a), $U_G = 2.82$ (b), and $U_G = 5.64$ (c). Experimental data fitting on each of the three substrate inhibition models was performed using nonlinear regression.

Table 4
Predicted values of the kinetic parameters for different models used in this study considering the ALR-NDT operating at the three superficial air velocities

	Haldane $(\mu = \mu_{max} S/(K_S + S + (\frac{S^2}{K_i}))$					Edwards $\left(\mu = \mu_{max} S/\left(K_S + S + (\frac{S^2}{K_i})(1 + \frac{S}{K})\right)\right)$						Aiba–Edwards $\left(\mu = \mu_{max} \frac{S}{K_S + S}\left(e^{\frac{-S}{K_i}}\right)\right)$				
	Constants			Goodness of fit		Constants				Goodness of fit		Constants			Goodness of fit	
Air flow rate (cm/s)	μ_{max} (1/h)	K_s (mg/L)	K_i (mg/L)	$S_{y.x}$	R^2	μ_{max} (1/h)	K_s (mg/L)	K_i (mg/L)	K (mg/L)	$S_{y.x}$	R^2	μ_{max} (1/h)	K_s (mg/L)	K_i (mg/L)	$S_{y.x}$	R^2
0.94	0.697	83.7	92.19	0.012	0.98	0.352	24.15	399.42	581.2	0.012	0.98	0.34	20.14	433.4[a]	0.011	0.98
2.82	0.772	100.4	77.2	0.008	0.99	–	–	–	–	–	–	0.347	22.4	408.9[a]	0.005	0.99
5.64	0.430	50.23	155.8	0.031	0.84	0.297	23.37	397.9	869	0.033	0.84	–	–	–	–	–

[a]K_i = 4.60 (mM) for U_G = 0.94 (cm/s) and K_i = 4.35 (mM) for U_G = 0.2.82 (cm/s).

Table 5
Kinetic parameters for phenol biodegradation

Culture	μ (1/h)	K_s (mg/L)	K_i (mg/L)	Refs.
Pseudomonas putida DSM 548	0.436[a]	6.19[a]	54.1[a]	[42]
Mixed	0.418[a]	2.9[a]	370[a]	[43]
Mixed	0.318[a]	57.35[a]	1503[a]	[44]
Mixed	0.306[a]	257.5[a]	162.6[a]	[45]
Mixed*	0.167[b]	95.05[b]	200[b]	[45]
Mixed	0.258[c]	200.3[c]	502[c]	[45]
Bacillus cereus strain AKG1	27.85[a]	59150[a]	2.411[a]	[46]
Bacillus cereus strain AKG1	925.6[c]	11530[c]	2355[c]	[46]
Bacillus cereus strain AKG1	0.470[b]	407[b]	431.3[b]	[46]
Bacillus cereus strain AKG2	1.635[a]	9.706[a]	3873[a]	[46]
Bacillus cereus strain AKG2	153.4[c]	1475[c]	4559[c]	[46]
Bacillus cereus strain AKG2	0.041[b]	125.88[b]	1117[b]	[46]

*K is the parameter described in the Edwards equation (see the text). The value of K for the mixed culture is 1,000 mg/L.
[a]refers to the Haldane equation and also [b,c]are corresponded to Edwards and Aiba–Edwards equations respectively.

assumptions originally made by the researcher for the model development: one assumption was based on the controlling role of the substrate diffusion into the cell (Eq. (7)) (growth stimulatory effect of substrate), and the other assumption was described as the presence of a protective mechanism through which limitation for the diffusion of the substrate into the cell becomes the rate-limiting step (such as high concentrations of substrate being growth inhibitory) (Eq. (8)) [5,40]:

$$\mu = \mu_{max} \frac{S}{S + K_s + \frac{S^2}{K_i}(1 + \frac{S}{K})} \quad (7)$$

$$\mu = \mu_{max}(e^{\frac{-S}{K_i}} - e^{\frac{-S}{K_S}}) \quad (8)$$

Among the test models used here, the latter form of the Edwards equation gave the poorest fit to the obtained data. Despite one additional fitting parameter (K) offered by Edwards model, little improvement in fitting experimental data was observed in Table 4 (i.e. the quality of data fitting in the form of the goodness of fit values). Further note on the growth inhibitory models was on the equation proposed by Aiba, which was described in the alcoholic fermentation process, based on the product inhibition assumption (Eq. (9)) [6]:

$$\mu = \mu_{max} \frac{S}{K_S + S}\left(e^{\frac{-P}{K_i}}\right) \quad (9)$$

According to the suggestion made by Edwards, the Aiba equation was extended to cover the growth inhibitory action of the substrate considering the involvement of common mechanisms in both the product and substrate inhibition cases [40] (Eq. (10)):

$$\mu = \mu_{max} \frac{S}{K_S + S}\left(e^{\frac{-S}{K_i}}\right) \quad (10)$$

The results of the study on phenol-degrading Pseudomonads possessing different phenol hydroxylases showed that the kinetic parameters calculated using the Aiba–Edwards equation (Eq. (10)) were interpretable in terms of K_i values [14]. The findings of the present work using Eq. (10) showed that *R. eutropha* tolerance toward phenol was higher compared with some strains, such as PC18 and PC69, with K_i in the range of 1.99–2.52 (mM) [14]. Satisfactory results of the goodness of fit indicated the preference of the Aiba–Edwards equation in the present study over the other test models (Table 4). Kovaravo-Kovar and Egli focused on the kinetic parameters and found that the cell behavior in a batch culture could be better characterized considering μ_{max} and not K_s and K_i [41].

There are large variations in the kinetic parameters for phenol biodegradation, and Table 5 presents a brief summary of the differences in the values reported in the literature.

4. Conclusions

The results presented in this study showed the potential of ALR-NDT for phenol biodegradation by *R. eutropha*. With reference to the hydrodynamic characteristics of the reactor, the positive effect of MSS on the ALR-NDT performance in terms of $\varepsilon_G t_m$, and $K_L a$ was reported, and the bubbles coalescence-inhibiting

property of the inorganic salts was confirmed. Equation $\varepsilon_G = aU_G^n$, as a familiar approach for expressing the dependence of ε_G on U_G, was used, and the bubbly flow regime in the ALR-NDT with the use of MSS was the favorable regime. The exponential dependence of K_La on U_G was also considered, and the value of K_La at ALR-NDT obtained for the air–MSS system was 1.2 times higher than that in the BCR and ALR at the highest U_G used in this work.

The variation of the experimental specific growth rate as a function of phenol concentration was determined using the nonlinear least squares technique. The Aiba–Edwards model, among the three substrate (growth) inhibition equations, gave the best fit. The effect of oxygen on phenol degradation was not considered to act as a growth-limiting substrate (not influential) because the aeration provided through ALR-NDT was sufficient to keep the oxygen concentration at a relatively constant level.

Acknowledgments

The authors express their thanks to Dr Samaneh Sanjari for her valuable assistance.

Nomenclature

ALR-NDT	—	airlift reactor with net draft tube
BCR	—	bubble column reactor
C_0	—	initial concentration of dissolved oxygen
C_s	—	saturated concentration of dissolved oxygen
C	—	bulk concentration of dissolved oxygen
H_L	—	liquid height before aeration
H_{LG}	—	liquid height after aeration
K_La	—	volumetric gas liquid mass transfer coefficient
K_s	—	half-saturation constant
K_i	—	inhibition constant
MSS	—	mineral salt solution
R^2	—	coefficient of determination
$S_{y.x}$	—	standard deviation of residuals
S	—	substrate concentration
S_0	—	initial phenol concentration
t_m	—	mixing time
U_G	—	superficial gas velocity
X	—	cell concentration
μ_{max}	—	maximum specific growth rate
ε_G	—	gas holdup

References

[1] H. Jamshidian, S. Khatami, A. Mogharei, F. Vahabzadeh, A. Nickzad, Cometabolic degradation of para-nitrophenol and phenol by *Ralstonia eutropha* in a Kissiris-immobilized cell bioreactor, Korean J. Chem. Eng. 30 (2013) 2052–2058.

[2] V. Arutchelvan, V. Kanakasabai, R. Elangovan, S. Nagarajan, V. Muralikrishnan, Kinetics of high strength phenol degradation using *Bacillus brevis*, J. Hazard. Mater. 129 (2006) 216–222.

[3] A. Habibi, F. Vahabzadeh, Degradation of formaldehyde at high concentrations by phenol-adapted *Ralstonia eutropha* closely related to pink-pigmented facultative methylotrophs, J. Environ. Sci. Health, Part A: Environ. Sci. Eng. Toxic Hazard. Subst. Control 48 (2013) 279–292.

[4] J.H. Tay, S.T.L. Tay, Y. Liu, K.Y. Show, V. Ivanov, Biogranulation Technologies for Wastewater Treatment: Microbial Granules, vol. 6, Elsevier, Oxford, 2006.

[5] A. Mulchandani, J. Luong, Microbial inhibition kinetics revisited, Enzyme Microb. Technol. 11 (1989) 66–73.

[6] J. Luong, Generalization of monod kinetics for analysis of growth data with substrate inhibition, Biotechnol. Bioeng. 29 (1987) 242–248.

[7] E. Jalilnejad, F. Vahabzadeh, Use of a packed-bed airlift reactor with net draft tube to study kinetics of naphthalene degradation by *Ralstonia eutropha*, Environ. Sci. Pollut. Res. 21 (2014) 4592–4604.

[8] S. Sanjari, F. Vahabzadeh, A. Naderifar, M. Pesaran, Hydrodynamics and mass transfer coefficients of airlift reactors with net draft tubes of different sizes: Production of cyclodextrin glucanotransferase using *Bacillus* sp., DSM 2523, Starch 66 (2014) 935–946.

[9] J. Merchuk, M. Gluz, in: M.C. Flickinger, S.W. Drew, Encyclopedia of Bioprocess Technology, John Wiley & Sons, Inc., New York, 2002, pp. 320–351.

[10] J. Merchuk, Why use air-lift bioreactors? Trends Biotechnol. 8 (1990) 66–71.

[11] Y. Chisti, U.J. Jauregui-Haza, Oxygen transfer and mixing in mechanically agitated airlift bioreactors, Biochem. Eng. J. 10 (2002) 143–153.

[12] W.T. Wu, J.Y. Wu, Airlift reactor with net draught tube, J. Ferment. Bioeng. 70 (1990) 359–361.

[13] D. Kuhn, M.A. Kholiq, E. Heinzle, B. Bühler, A. Schmid, Intensification and economic and ecological assessment of a biocatalytic oxyfunctionalization process, Green Chem. 12 (2010) 815–827.

[14] S. Viggor, E. Heinaru, A. Künnapas, A. Heinaru, Evaluation of different phenol hydroxylase-possessing phenol-degrading pseudomonads by kinetic parameters, Biodegradation 19 (2008) 759–769.

[15] M. Motamedi, A. Habibi, M. Maleki, F. Vahabzadeh, Kinetic Modeling of p-nitrophenol and phenol by kissiris-immobilized *Ralstonia eutropha* in a batch reactor, Clean—Soil Air Water 42 (2014) 1–7.

[16] E. Jalilnejad, A. Mogharei, F. Vahabzadeh, Aerobic pretreatment of olive oil mill wastewater using *Ralstonia eutropha*, Environ. Technol. 32 (2011) 1085–1093.

[17] D.Y. Hsiun, W.T. Wu, Mass transfer and liquid mixing in an airlift reactor with a net draft tube, Bioprocess Eng. 12 (1995) 221–225.

[18] Y.J. Tang, J.J. Zhong, Role of oxygen supply in submerged fermentation of *Ganoderma lucidum* for production of *Ganoderma* polysaccharide and ganoderic acid, Enzyme Microb. Technol. 32 (2003) 478–484.

[19] J.E. Bailey, D.F. Ollis, Biochemical Engineering Fundamentals, McGraw Hill, New York, NY, 1986.

[20] J. Box, Investigation of the Folin-Ciocalteau phenol reagent for the determination of polyphenolic substances in natural waters, Water Res. 17 (1983) 511–525.
[21] L.L. Lapin, Modern Engineering Statistics, Duxbury Press, Belmont, California, 1997.
[22] C.P. Chen, S.J. Yang, W.T. Wu, A novel rectangular airlift reactor with mesh baffle-plates, Biotechnol. Tech. 11 (1997) 439–441.
[23] J. Snape, M. Fialova, J. Zahradnik, N.H. Thomas, Hydrodynamic studies in an external loop airlift reactor containing aqueous electrolyte and sugar solutions, Chem. Eng. Sci. 47 (1992) 3387–3394.
[24] D.J. McClements, Food Emulsions: Principles, Practices, and Techniques, CRC Press, Florida, 2004.
[25] K. Schügerl, J, Lücke, J. Lehmann, F. Wagner, in: T. K. Ghose, A. Fiechter, N. Blakebroug, Advances in Biochemical Engineering, Springer-Verlag, Heidelberg 1978, pp. 63–131.
[26] R.R. Lessard, S.A. Zieminski, Bubble coalescence and gas transfer in aqueous electrolytic solutions, Ind. Eng. Chem. Fundam. 10 (1971) 260–269.
[27] H. Hikita, S. Asai, K. Tanigawa, K. Segawa, M. Kitao, Gas hold-up in bubble columns, Chem. Eng. J. 20 (1980) 59–67.
[28] H. Nikakhtari, G.A. Hill, Hydrodynamic and oxygen mass transfer in an external loop airlift bioreactor with a packed bed, Biochem. Eng. J. 27 (2005) 138–145.
[29] H.L. Tung, S.Y. Chiou, C.C. Tu, W.T. Wu, An airlift reactor with double net draft tubes and its application in fermentation, Bioprocess Eng. 17 (1997) 1–5.
[30] O. Tepe, A.Y. Dursun, Combined effects of external mass transfer and biodegradation rates on removal of phenol by immobilized *Ralstonia eutropha* in a packed bed reactor, J. Hazard. Mater. 151 (2008) 9–16.
[31] M.C. Tomei, M.C. Annesini, S. Bussoletti, 4-nitrophenol biodegradation in a sequencing batch reactor: Kinetic study and effect of filling time, Water Res. 38 (2005) 375–384.
[32] D. Leonard, C.B. Youssef, C. Destruhaut, N.D. Lindley, I. Queinnec, Phenol degradation by *Ralstonia eutropha*: Colorimetric determination of 2-hydroxymuconate semialdehyde accumulation to control feed strategy in fed-batch fermentations, Biotechnol. Bioeng. 65 (1999) 407–415.
[33] S. Aiba, A.E. Humphrey, N.F. Millis, Biochemical Engineering, second ed., Academic Press, New York, NY, 1973.
[34] S. Simkins, M. Alexander, Models for mineralization kinetics with the variables of substrate concentration and population density, Appl. Environ. Microbiol. 47 (1984) 1299–1306.
[35] K.V. Shetty, I. Kalifathulla, G. Srinikethan, Performance of pulsed plate bioreactor for biodegradation of phenol, J. Hazard. Mater. 140 (2007) 346–352.
[36] W. Brunner, D.D. Focht, Deterministic three-half-order kinetic model for microbial degradation of added carbon substrates in soil, Appl. Environ. Microbiol. 47 (1984) 167–172.
[37] J.F. Andrews, A mathematical model for the continuous culture of microorganisms utilizing inhibitory substrates, Biotechnol. Bioeng. 10 (1968) 707–723.
[38] I.S. Kim, H. Lee, J.T. Trevors, Effects of 2, 2´, 5, 5´-tetrachlorobiphenyl and biphenyl on cell membranes of *Ralstonia eutropha* H850, FEMS Microbiol. Lett. 200 (2001) 17–24.
[39] G. Schüürmann, R.K. Somashekar, U. Kristen, Structure activity relationships for chloro-and nitrophenol toxicity in the pollen tube growth test, Environ. Toxicol. Chem. 15 (1996) 1702–1708.
[40] V.H. Edwards, The influence of high substrate concentrations on microbial kinetics, Biotechnol. Bioeng. 12 (1970) 679–712.
[41] K. Kovárová-Kovar, T. Egli, Growth kinetics of suspended microbial cells: From single-substrate-controlled growth to mixed-substrate kinetics, Microbiol. Mol. Biol. Rev. 62 (1998) 646–666.
[42] Á.A. Monteiro, R.A. Boaventura, A.E. Rodrigues, Phenol biodegradation by *Pseudomonas putida* DSM 548 in a batch reactor, Biochem. Eng. J. 6 (2000) 45–49.
[43] A.G. Livingston, H.A. Chase, Modeling phenol degradation in a fluidized-bed bioreactor, AIChE J. 35 (1989) 1980–1992.
[44] A. Lallai, G. Mura, R. Miliddi, C. Mastinu, Effect of pH on growth of mixed cultures in batch reactor, Biotechnol. Bioeng. 31 (1988) 130–134.
[45] S. Dey, S. Mukherjee, Performance and kinetic evaluation of phenol biodegradation by mixed microbial culture in a batch reactor, Int. J. Water Resour. Environ. Eng. 2 (2010) 40–49.
[46] A. Banerjee, A.K. Ghoshal, Phenol degradation by *Bacillus cereus*: Pathway and kinetic modeling, Bioresour. Technol. 101 (2010) 5501–5507.